Tartaruga, I., Cooper, J., Lowenberg, M., & Lemmens, Y. (Accepted/In press). Enhanced evolutionary-based optimization techniques applied to a nonlinear landing gear design problem. *Journal of Aircraft*.

Peer reviewed version

Enhanced evolutionary-based optimization techniques applied to a nonlinear landing gear design problem

I. Tartaruga [a]
University of Bristol, Department of Engineering Mathematics

J. E. Cooper [b], M. H. Lowenberg [c]
University of Bristol, Department of Aerospace Engineering,

Queens Building, University Walk, Bristol, United Kingdom, BS8 1TR

Y. Lemmens [d]
Siemens PLM Software, Aerospace Competence Center, Leuven, Belgium

Engineering design processes often use optimization strategies, which aim to minimize multi-objective functions. The analysis should consider the uncertainty in a system, which may cause significant changes in its behaviour. The inclusion of the uncertainty in the design process makes the identification of an optimum design more challenging. In this paper, two novel optimization methods (Iterative Differential Evolutionary Algorithm - I.D.E.A. and Reliable & Robust Evolutionary Algorithm - R.R.E.A.) are presented. These optimization strategies aim to solve problems that are very time demanding and for which it is difficult (and expensive) to determine derivatives and to identify and define the optimum set of parameters. The approaches are validated considering as a test case the optimization of a landing gear system in order to avoid the onset of shimmy, assuring a reliable design.

[a] Research Associate, University of Bristol, irene.tartaruga@bristol.ac.uk .
[b] RAEng Airbus Sir George White Professor of Aerospace Engineering, Dept of Aerospace Engineering, University of Bristol, J.E.Cooper@bristol.ac.uk.
[c] Professor of Flight Dynamics, Dept of Aerospace Engineering, University of Bristol, M.Lowenberg@bristol.ac.uk.
[d] Sr Project Leader RTD, Siemens PLM Software, yves.lemmens@siemens.com.

Nomenclature

Methodology Notation

$count_G$ = number of evaluated generations in the differential evolutionary algorithm

CR = crossover variable in the differential evolutionary algorithm

d = direction of interest

$f(\mathbf{x})$ = objective function

$\mathbf{F}^*$ = set of values for the input factor such that the relative locus of interest LoI is tangent to the defined limit-state function g

$\mathbf{F}_G$ = set of values of the input factor at the generation G

F = scale factor in the differential evolutionary algorithm

g = limit-state function

N_G = number of generation

G_{max} = maximum number of generations in the differential evolutionary algorithm

HB = Hopf Bifurcation

$h_p^{\pm}$ = quantity adopted in URQ

i, k = indices for each step of the continuation analysis and for the continuation algorithm iterations to converge to steady solutions

LoI = locus of interest in the optimization process

$N_{max_{Feval}}$ = maximum number of function evaluations in the differential evolutionary algorithm

NP = number of populations (N-dimensional vectors) in a generation

$P_{max_{ineg,pos}}$ = the maximum negative and positive range of variation for the ith considered parameter ($i = 1...N$)

r_1, r_2, r_3, r_4, r_5 = random factors in the differential evolutionary algorithm

S = coefficient adopted for one of the objective functions in the R.R.E.A. technique

Tol_ϵ, Tol_p = tolerances in the I.D.E.A. iterative process

$\mathbf{v}_{i,G}$ = mutant vector in the differential evolutionary algorithm

VTR = desired value to search in the optimization process

$W_0, W_p, W_p^+, W_p^-, W_p^{\pm}$ = weights adopted for the URQ

$\mathbf{x_{best,G}}$ = best vector determined for the generation G in the differential evolutionary algorithm

$\mathbf{x}_{r_k,G}$ = r_k vector at the generation G in the differential evolutionary algorithm

$\mathbf{x}$, $\mathbf{P}$ = independent states and bifurcation parameters in the bifurcation analysis

$x_1, x_2, ..., x_N$ = components for the input design factor vector $\mathbf{x}$

ϵ = relative acceptable error

μ_x, σ_x^2, γ_x, Γ_x = input statistical quantities: mean, variance, skewness and kurtosis

μ_d, σ_d = mean and deviation of the output of interest

τ_F, τ_{CR} = constants to perform self-adaptation in the differential evolutionary algorithm

Landing gear model notation

B_m = track of the main assembly

B = distance between the nose and the axis of the main assembly

c_ψ = damping for the torsional degree of freedom

I_ψ = moment of inertia for the torsional degree of freedom

L = tyre relaxation length

L_δ = distance L_δ from the axle about which the rotational degree of freedom δ is considered

L = lift

V = forward velocity

W = weight of the aircraft

β = out-of-plane rotational degree of freedom

δ = in plane rotational degree of freedom

λ = lateral tyre displacement

ϕ = rake angle

ψ = torsional degree of freedom describing the rotation of the wheel/axle assembly about the local axis z

Abbreviation

HC = Hypercube

I.D.E.A. = Iterative Differential Evolutionary Algorithm

LCO = Limit Cycle Oscillation

LoI = Locus of Interest

MCS = Monte Carlo Simulations

PDF = Probability Density Function

QoI = Quantity of Interest

ROM = Reduced Order Model

RBDO = Reliability-Based Design Optimization

RDO = Robust Design Optimization

R.R.E.A. = Reliable & Robust Evolutionary Algorithm

SA = Sensitivity Analysis

SVD = Singular Value Decomposition

URQ = Univariate Reduced Quadrature

I. Introduction

Optimization techniques are commonly adopted for a system analysis with the aim of validating and evaluating a system already designed or to actually define the design that fulfils some fixed requirement. A range of optimization methods can be used and the selection depends on the goal of the optimization itself: the sought optimum can be required to be either reliable or robust, or both reliable and robust. Robustness refers to the *minimization of the variance* in the determined optimum, while reliability concerns the *minimization of the occurrence* of limit-state or constraint violations ([1]). Loci of solution points describing specific variations of quantities of interest are considered during an optimization of a structure that aims to assure reliability by minimizing the probability of failure.

Technological progress often leads to an increase in the complexity of systems of interest and application of optimization techniques to complex systems can be challenging. This complexity

requires the development of techniques able to deal with the design of such systems. In the aeronautical field the complexity may arise due to the presence of a very large number of subsystems, such as flight controls, electrical systems, landing gear, avionics system, instrumentation and recording, etc. The source of complexity can be due to the number of components and their geometry as well as the non-linearities characterizing the system dynamics and the description of quantities of interest for the analysis. In this scenario, complexity can be due to the description of the variation of the quantities of interest (which we refer to as 'locus of interest') that is needed to assure the limiting criteria to be fulfilled and, whatever the method of analysis, the determination of an optimum design can be difficult. Moreover, the difficulty during the optimization process increases if uncertainty, which is always present in all branches of physics and engineering, is included in the analysis. This effect is particularly true for systems whose numerical model is computationally expensive to evaluate.

In the optimization process, uncertainty in the system has not always been considered and instead a deterministic process is adopted ([2–5]), typically incorporating a safety factor ([6]). The consideration of uncertainties in the development and improvement of optimization processes has recently become of significant interest ([7]). In fact, there is awareness within the engineering sector that a deterministic approach, with the application of a safety factor, often results in an over or under designed system ([1]).

Techniques that are commonly adopted to optimize a system under uncertainties ([8], [1]) are Robust Design Optimization (RDO) ([9]) and Reliability-Based Design Optimization (RBDO) ([10]). In RDO the mean of the response of interest is optimized by minimizing its variance. In RBDO, a cost function is minimized and the uncertainty is considered, introducing specific risk and target reliability constraints that require tail statistics to be computed. In the presence of a very computationally expensive numerical model, nonlinear behaviour and multi-objective problems, the traditional RDO and RBDO aproaches are not always suitable because of two main issues: the prohibitive computational cost and the neglect of higher-order moments commonly used for the RDO and RBDO techniques. If a finite element model (FEM) or multi-body model is considered, the analysis is simplified as much as possible and non-linear stability analysis is usually not considered;

the focus may be on fatigue life([11]), stress and shape optimization ([12], and linear stability ([2]). The reason for such a choice is the significant computational time required if non-linear analysis is considered and the difficulties in automatically tracking and parametrizing the response of interest for further analyses.

The complexity of a problem can be reduced thanks to the adoption of specific techniques. The first step is to identify the quantities that are of interest for the analyzed problem; the label QoI is here used as abbreviation for these entities. The factors that most influence the system can be isolated using sensitivity analysis techniques ([13]). Then, surrogate models and reduced order models (ROMs) can be constructed in terms of the identified factors and QoI. Finally, using the ROMs and suitable strategies to perform optimization and to propagate uncertainties, possible optimum designs need to be critically assessed in terms of the defined objective functions and requirements, considering the most influential factors as uncertain and/or design variables and applying suitable optimization strategies.

Currently, available optimization methodologies have a limited capability to deal with objective functions that are very computationally expensive and affected by non-linear phenomena. In particular, the limitation is in terms of methods that can assure reliability, and possibly robustness, sufficient for an engineering structure whose analysis is time demanding even in the absence of uncertainty. Alternative optimization strategies have been proposed to overcome these problems, aggressive design procedures ([7, 14]), to make feasible the probabilistic design ([15, 16]). The main idea behind aggressive design techniques is to exploit the existence of a desired target; a desired nominal response of interest and its statistical properties are defined and the optimization is then performed such that the sought target-desired performance is matched as closely as possible ([7, 14]). The difficulty in such an approach, is that, depending on the problem, it is not assured that the desired target is matched 'close' enough or that the computational effort is actually reduced. In this scenario, the necessity arises to develop a method that can assure reliability and possibly also robustness for an engineering structure whose analysis is time demanding even in the absence of uncertainty.

The original contribution of this paper is to provide optimization techniques that can:

- be considered when objective functions are expensive to compute and involve correlated quantities, in particular if the system is non-linear;
- limit the number of evaluations of the objective function and hence the computational cost of the nonlinear analysis;
- guarantee a minimization of the probability of failure while limiting the dependence on approximations to evaluate the objective functions of interest;
- identify the maximum range of parameter variation for the investigation;
- avoid gradient calculations;
- produce reliable and/or robust solutions.

Two optimization techniques have been developed and are presented here: the first (Iterative Distribution Evolutionary Algorithm - I.D.E.A.) is a reliability - based method, while the second (Robust and Reliable Evolutionary Algorithm - R.R.E.A.) can be tuned in order to achieve a more reliable or robust optimum. R.R.E.A. calculates the statistical quantities, using Univariate Reduced Quadrature ([17]) to reduce computational cost. Both the optimization techniques aim to limit the number of evaluations of the objective function without involving approximations in the computation, guarantee a minimization of the probability of failure, and avoid gradient calculations. The developed strategies are applied to the selection of design variables in a landing gear system featuring complex nonlinearity in its dynamics subjected to structural uncertainties. The goal of the considered application is to decrease the probability of occurrence of 'shimmy' - a self-sustained oscillation resulting from the nonlinear interaction between the follower forces acting on the tyre and the modes of vibration - during ground manoeuvres. In this paper, the methodology and landing gear model are described next, followed by its implementation and presentation of results; conclusions are then drawn from the study.

II. Methodology

An optimization problem is formulated as follows. A vector of values $x_1, x_2, ..., x_N$ for an input design factor vector $\mathbf{x}$ is sought in order to minimize the defined objective function $f(\mathbf{x})$. The design factors are selected among a number of factors, each influencing to a certain degree the output of interest for the optimization. The selection is performed using sensitivity analysis (SA) techniques, in this case Sobol' indexes [13, 18, 19].

In the proposed optimization strategies, the nominal values of the selected design factors are regarded as uncertain. However, there is no limitation in the choice of design/uncertain factors that can be considered. The strategies are conceived in order to solve problems that are very time demanding and for which it is difficult (and expensive) to determine derivatives and to identify and define the optimum set of parameters. The achieved reduction in computational time is both in terms of number of cases to be analyzed directly through experiments or runs of numerical models, and in avoiding the computations of gradients. The completeness of the analysis is fulfilled thanks to the inclusion of efficient and effective methodologies to perform SA and propagate uncertainties in the system.

The two novel optimization methods are: the Iterative Distribution Evolutionary Algorithm, I.D.E.A., and Reliable & Robust Evolutionary Algorithm, R.R.E.A. . They both consist of three phases and can be categorized as evolutionary algorithms ([20–22]). Evolutionary Algorithms (EAs) are population-based metaheuristic optimization algorithms that explore the set of possible solutions for a sufficient set of solutions following a mechanism inspired by biological evolution, namely reproduction, generation, mutation, recombination and selection. The optimization considers the input factors as individuals belonging to populations that are generated through mutation and recombination and that can be subjected to mutation. EA techniques are extremely versatile since they can be adopted to any problem of interest, since no assumptions are made ([23]) and their efficiency has been recognised in the industrial environment [24] . However, the determined solution is numerical and is an approximation of the unknown optimal one, which means that it could be sub-optimal. In this scenario, it is important to remark that in engineering problems an optimum result can be difficult to identify and is not uniquely defined and thus evolutionary algorithms are

effective.

The proposed optimization algorithms are innovative procedures that aim to minimize the probability of failure without directly computing it due to the unfeasible computational cost in obtaining the probability density function of the quantity of interest. I.D.E.A. aims to determine the range of variation for the input factors for which the uncertain boundary is tangent to the limit condition for the reliable area. It also provides an understanding of the acceptable range of uncertainties exploiting geometrical considerations to distribute the points to be investigated in the considered parameter space. The method does not build on pre-existing techniques and is a new strategy. R.R.E.A. aims to assure reliability and/or robustness to the design, minimizing the objective function defined in terms of the mean μ_d and deviation σ_d of the output of interest. Three cases, i.e. three objective functions, have been analyzed and the difference is due to the main goal of the optimization:

1. $f(\mathbf{x}) = \mu_d + S\sigma_d$, the critical uncertain boundary is kept as big a distance as possible from the limit condition for the reliable area (*conservative condition*)

2. $f(\mathbf{x}) = |\mu_d + S\sigma_d|$, the uncertain boundary is tangent to the limit condition for the reliable area (*non conservative condition*);

3. $f(\mathbf{x}) = \sigma_d$; the most robust solution is sought.

The optimization code allows the goal to be reached, combining existing formulae to approximate μ_d and σ_d. A differential evolutionary algorithm, enhanced by the authors, has been considered to define the overall structure of the method. The differential evolutionary technique is a self-adaptive one, which has been introduced in [25] and denoted as jDE. The differential evolutionary algorithm was originally proposed by Storn and Price ([26]) as a population-based algorithm to be adopted in order to perform global optimization in the presence of continuous domains. A Differential Evolutionary algorithm is quite simple to implement, it is robust and belongs to the most powerful group of evolutionary algorithms ([20–22, 25]). The optimization strategy has been developed in order to minimize the stated objective functions. Moreover, approximated formulae have been considered for the mean μ_d and the standard deviation σ_d of the output of interest due to the lack of a closed-form

solution of the integrals that need to be evaluated to compute the statistical quantities

$$\mu_d = E\left[f(\mathbf{x})\right] = \int_{-\inf}^{+\inf} f(\mathbf{x}) p_{\mathbf{x}}(\mathbf{x}) d\mathbf{x} \tag{1}$$

$$\sigma_d^2 = E\left[\left(f(\mathbf{x}) - \mu_d\right)^2\right] = \int_{-\inf}^{+\inf} \left[f(\mathbf{x}) - \mu_d\right]^2 p_{\mathbf{x}}(\mathbf{x}) d\mathbf{x}$$

In what follows the approach considered to identify the range of variation to start the optimization process is presented; it is the first step common to both the proposed optimization strategies and it constitutes the first two phases. Then, the residual phases applicable to the Iterative Distribution Evolutionary Algorithm and Reliable & Robust Evolutionary Algorithm are presented. Finally, the minimization of functions usually used to test optimization algorithms is performed in order to compare the differential evolutionary algorithm and the enhanced one, developed by the authors.

A. Range of Factor Variation for the Optimization Process

The Iterative Distribution Evolutionary Algorithm and the Reliable & Robust Evolutionary Algorithm consist of three phases. The starting step for the iterative procedure is to identify the set of values for the parameters $\mathbf{F}^*$.

The stated identification can be performed once some directions of interest have been defined for the analysed problem. The directions of interest lie in the same space as the locus of interest *LoI* and the limit-state function g; the stated space has the dimensions equal to the the number of quantities of interest (QoI) and in the present paper it is a two-dimensional space since two are the QoI for the analysed problem. The locus of interest is the collection of the values of the QoI identifying a certain behaviour of interest, while the limit-state function collects the values of the QoI that define the limit of the failure region (Figure 1). The direction of interest need to be defined by the researcher in the best way to capture the probabilistic characteristics. For instance, in the presence of uncertainties that determine a delimited uncertain area for the *LoI*, then the directions of interest can be defined as the lines that connect points between lower and upper bounds of the stated uncertain area. The points can be determined by discretizing the lower and upper bounds.

Having obtained the direction of interest, the set of values for the parameters $\mathbf{F}^*$ can then be defined in one of the following ways:

- such that the locus of interest LoI is tangent to the defined limit-state function g.
- identifies the direction of interest for which the probability of failure is highest (that will be labelled as direction d); the set is the one for which the distance between the relative locus of interest LoI and the limit-state function g is a minimum.

Both of these methods have been considered since it is possible that for some cases of interest the described tangency doesn't occur.

The locus of interest and the limit-state function are functions of the quantities of interest of the analysed problem. For the sake of clarity Figure 1 show an example for the stated scenarios.

In Figure 1, the considered generic problem is defined in terms of two quantities of interest (QoI_1 and QoI_2). In the considered generic problem the directions of interest are connecting same indexed points of the discretized loci of interest, which are laying in the space defined by the quantities of interest (QoI).

In Figure 1, three directions are shown for simplicity, and the probability of failure is also presented along these three directions of interest. In this example, the failure occurs when a point on the locus of interest lies in the convex space delimited by the limit state function. Three loci are shown in the figures; the set of values for the parameters $\mathbf{F}^*$ is identified among all the values $\mathbf{F}$ adopted. Each set $\mathbf{F}$ is linked to a specific locus of interest since the quantities of interest describing such a locus are determined by a specific set $\mathbf{F}$. Figure 1 shows the case for which the tangency between a locus of interest and the limit state function occurs, thus the set $\mathbf{F}^*$ is the one that generates such a locus of interest. The same Figure 1 can be used also to show how to identify the set $\mathbf{F}^*$ considering only the direction for which the probability of failure is highest; along this direction the distance from the limit state function of each considered locus is determined and the set $\mathbf{F}^*$ is given by the one related to the state function characterized by a minimum distance.

In what follows the first two phases common to I.D.E.A. and R.R.E.A. are presented.

First phase: Preparation The objectives of the optimization are established including possible acceptable tolerances. In particular, the limit state function g that delimits the failure region has to be defined. Moreover, in the presence of a system with many parameters sensitivity analysis needs

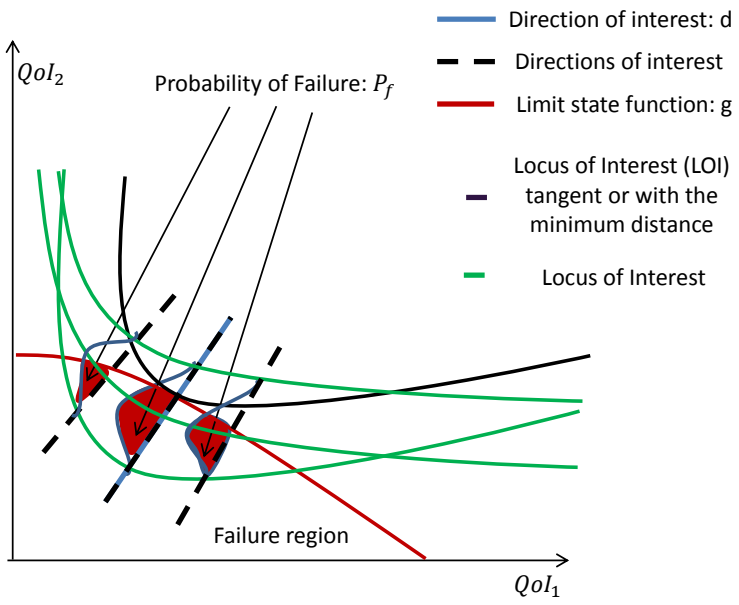

Fig. 1: Selection of $\mathbf{F}^*$ looking at the probability of failure or considering the distance between the locii and the limit state function g along the direction of interest d.

to be performed to detect the most influential ones for the considered objectives in the optimization process. Sobol indices ([13, 18]) are adopted. Having identified the parameters to be considered during the optimization process, the maximum negative and positive ranges of variation $P_{max_{i_{neg,pos}}}$ for the ith considered parameter ($i = 1...N$) are defined. In case a symmetric variation of the parameter of interest is adopted, then $P_{max_{i_{neg}}}$ is equal to $P_{max_{i_{pos}}}$ and the maximum percentage is P_{max_i}.

Second phase: Data Collection The quantities of interest (QoIs), those that describe the locus of interest and limit-state function, are evaluated for a suitable number of points in the parameter space by directly running the numerical model or doing experiments. These are needed to train surrogate models adopted in the SVD based methodology ([27–30]). Using the SVD/metamodelling based methodology can reduce by 95% the time required to investigate the parameter space to determine the set of nominal values $\mathbf{F}^*$ for which the stated tangency occurs. Knowing $\mathbf{F}^*$, the intervals $(x_{j,low}, x_{j,upp})$ of interest for each jth design parameter are selected such that the point $\mathbf{F}^*$ is internal to the final optimum uncertain interval of variation and is around the optimum nominal value $\overline{\mathbf{F}}_{opt}$. If $\mathbf{F}^*$ is selected considering the tangent condition, it is worth noticing that the analyses are per-

formed numerically, thus the tangency can be defined as the state for which the locus of interest LoI is the nearest one to the defined limit function g along the direction of interest d previously identified. Mathematically, this can be expressed as $\mathbf{F}^* := \mathbf{F}|(dist(g - LoI(\mathbf{F}^*)_d) = \min(dist(g - LoI(\mathbf{F})_d)$.

1. Determine the upper and lower bounds for the optimum nominal value. Given that the point $\mathbf{F}^*$ needs to be internal to the final optimum uncertain interval of variation, the stated bounds are defined as by eqs. (2) and (3).

$$\overline{\mathbf{F}}_{opt_{upp}}(1 - P_{max_{i_{low}}}) = F_i^* \tag{2}$$

$$\overline{\mathbf{F}}_{opt_{low}}(1 + P_{max_{i_{upp}}}) = F_i^* \tag{3}$$

2. Define the maximum possible interval of variation for the lower or upper nominal value $\overline{\mathbf{F}}_{opt}$ such that

$$[\overline{\mathbf{F}}_{opt_{low}}(1 - P_{max_{i_{low}}}), \overline{\mathbf{F}}_{opt_{upp}}(1 + P_{max_{i_{upp}}})] \tag{4}$$

3. Substitute the lower and upper bounds of eqs. (2) and (3) into (4) to give the required expression

$$[F_i^* \cdot \frac{1 - P_{max_{i_{low}}}}{1 + P_{max_{i_{upp}}}}, F_i^* \cdot \frac{1 + P_{max_{i_{upp}}}}{1 - P_{max_{i_{low}}}}] \tag{5}$$

The range of variation defined in eq. (5) is the same for both the optimization strategies.

The user can decide to consider more than one set $\mathbf{F}^*$ to continue the optimization process and eventually pick the best set according to other requirements, such as robustness.

In the following subsections the other phases needed to complete the proposed optimization processes are presented.

B. Iterative Distribution Evolutionary Algorithm

The Iterative Distribution Evolutionary Algorithm has the capability of minimizing the probability of failure (a *reliable optimizer*) and providing an understanding of the acceptable range of uncertainties. I.D.E.A. consists of three phases: the first two have been already presented in section II A and Figure 2 presents the flow chart describing the last phase, which is iterative. In Figure 2 HC is an abbreviation of hypercubes.

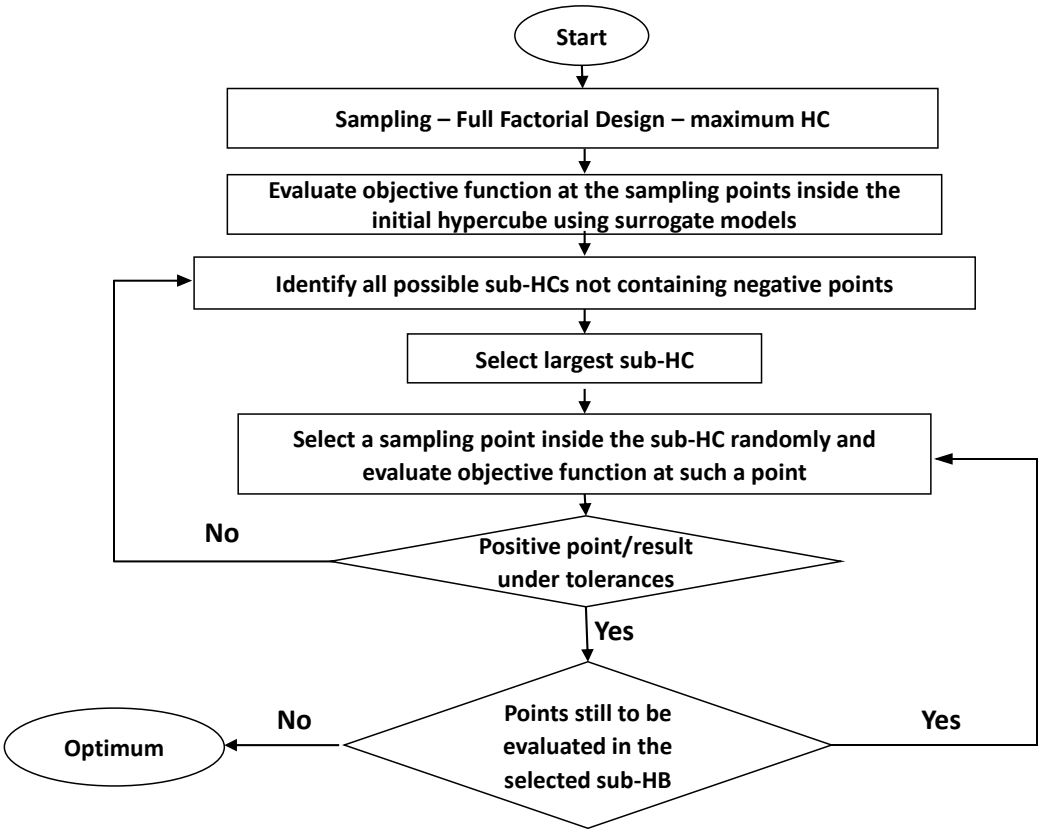

Fig. 2: Flow chart describing the iterative phase of the I.D.E.A..

Third phase: Iterative Process The third phase is the iterative part that has evolutionary characteristics. A general evolutionary algorithm has three main steps: generation, mutation and selection ([20–22]). Each generation consists of separate selection and mutation steps performed iteratively. In IDEA the generation is the region-hypercube of interest identified for each set $\mathbf{F}^*$ the user wants to use; this hypercube has as many dimensions as the number of design factors and

each value of the design factors is delimited by the defined interval (eq. (5)). Moreover, for each generation, a full factorial design is considered to define sampling points in which to evaluate the objective function. This consists of generating a well structured sampling plane that has the aim to not exclude any values for a specific parameter that could match desired requirements for some precise values of other parameters. For each generation and each point in the full factorial sampling plane, the QoI need to be evaluated. Thanks to the surrogate models already trained, a saving in time can be achieved. The surrogate models are used to evaluate the QoI at the points that are in the range considered in the first phase. Depending on the obtained QoI the points are divided into two groups: positive and negative. The positive points are those for which the loci identified by the QoI are not in the failure region or if they are, the defined tolerance Tol_ϵ is fulfilled such that

$$dist(g - LoI(\mathbf{F}_G)_d) - dist(g - LoI(\mathbf{F}^*)_d) <= Tol_\epsilon \cdot dist(g - LoI(\mathbf{F}^*)_d) \tag{6}$$

where G is used here to emphasize belonging to a particular generation; $\mathbf{F}_G$ is the set of values of the parameters at the generation G.

All the other points are negative and always present since, as previously stated, the optimization process is considered for problems that do not have an acceptable probability of failure.

The mutation consists of a subdivision of the hypercube along particular directions such that all the new hypercubes contain the point $\mathbf{F}^*$. The directions for the subdivisions are identified by the negative set of points, and in particular by the values assumed by the parameters at such a point. The directions are identified by varying all the parameters at the negative point but one. The number of the directions for each negative point is equal to the dimension of the hypercube, i.e. the number of design parameters.

To perform the subdivision, the set of points inside the hypercube are defined such that the directions are parallel to the sides of the hybercube. In fact, in this way, fixing the values of all the design factors but one, the direction containing negative points can be identified. Thus, the full factorial design is the selected sampling strategy only for subdivision purposes (the Latin Hypercube Sampling method is adopted to train the surrogate models).

Figure 3 clarifies the procedure considering an hypercube in 2D (the black rectangle) and just one negative point (the yellow point). The black rectangle is always the same initial hypercube and

all the possible subdivisions are shown. The blue rectangles are those to be neglected ('positive' points) and the red rectangles are considered to improve the optimization further ('negative' points). Moreover, in Figure 3 the green and yellow points are the one related to the set $\mathbf{F}^*$ and belonging to the negative set. At the end of the mutation step, no hypercube with negative points inside should be present.

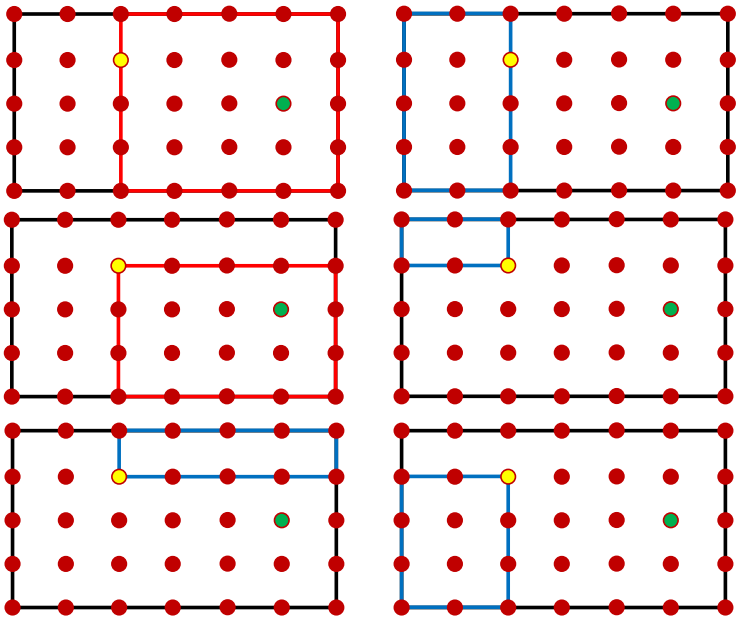

Fig. 3: Example of the mutation strategy.

The selection step consists of sorting the hypercube in a descending order in terms of the volume and evaluating the QoI at the points not in the range considered in phase one. This selection can only be done by directly running the numerical model or using experimental results. Finally, the selected hypercube in the one that does not have a tolerance greater than Tol_p of points for which the loci of interest are intersecting the limit state function, accepting also the tolerance shown in eq. (6). Tol_p is defined as the percentage of the number of negative points acceptable in the hypercube with respect to the total number of points belonging to the considered hypercube. The optimum set of values is assumed to be the mean point in the hypercube.

Validation phase The optimum sets of values determined for each generation can be compared, performing uncertainty quantification (UQ) for each of them and looking at the results. This comparison can be accomplished either using just the points belonging to the optimum hypercube or

adopting SVD based methods. The desired optimum set is the one that provides the minimum probability of failure (high reliability) and the least width of PDF (high robustness) or a suitable defined compromise of these properties. Once the optimum is found, the nominal value and percentage variation can be defined as preferred, i.e. assuming a symmetric or asymmetric distribution.

C. Reliable & Robust Evolutionary Algorithm

The Reliable & Robust Evolutionary Algorithm has the capability of minimizing the objective function of interest $f(\mathbf{x})$ defined in terms of the mean μ_d and standard deviation σ_d, (case 1: $f(\mathbf{x}) = \mu_d + S\sigma_d$, case 2: $f(\mathbf{x}) = |\mu_d + S\sigma_d|$, case 3: $f(\mathbf{x}) = \sigma_d$). Looking at the selected objective function, the expectation is that the higher the value of the coefficient S, the more the optimization tries to minimize the other statistical quantity, σ_d. However, this can also be untrue if, for instance, the coefficient S is increased and the required minimization can then be fulfilled by decreasing the mean without the need to reduce the variance with respect to that related to a higher value of S. Comparing the two optimization methods, the non-conservative condition (i.e. the tangent-limit condition - case 2 for the R.R.E.A.) is the result that can be obtained using the I.D.E.A. process, while more or less conservative results can be obtained using the R.R.E.A. method. If the tangent-limit condition is the desired objective then both methods can be used only if the input statistical quantities are known; if such information is lacking the I.D.E.A. process must be used instead. In fact, the R.R.E.A. method approximates the output statistical quantities, which require the first four input statistical quantities to be known (i.e. the mean μ_x, the variance σ_x^2, the skewness γ_x and the kurtosis Γ_x).

The R.R.E.A. method consists of three phases; the first two have been already presented in II A, and the last one is discussed here.

Third phase: Optimization The last phase of the algorithm is the core of the optimization. In order to determine the set of values of the input factors that minimizes the selected objective function a technique to approximate the statistical quantities has been used and an evolutionary algorithm has been considered. The approximated statistical quantities have been determined using the Univariate Reduced Quadrature technique (URQ) ([17, 31]). URQ belongs to the categories of numerical approximation techniques to compute the integrals that define the stated statistical

quantities (eq.(1)) such as Taylor-based Moment Propagation, Gaussian Quadrature, Monte Carlo Simulations (MCS) and Statistic Expansion. The URQ technique provides formulas consisting of sums of functional values that try to match the highest possible number of terms of the mean and variance expressions based on a third order Taylor-series expansion. The URQ has the advantage of having one less level of differentiation if compared to the methods based on first derivatives, thus it is advantageous with respect to gradient-based optimization techniques. The URQ method has a higher accuracy than those characterizing the linearization method, but similar computational cost. This has been shown in [17] by using a fourth-order Taylor-series expansion. The use of such a technique requires the first four moments of the input uncertain parameters to be known, i.e. the mean μ_x, the variance σ_x^2, the skewness γ_x and the kurtosis Γ_x. Adopting the URQ method, the output statistical quantities can be determined by evaluating the objective function at $2n+1$ points (n is the number of uncertain input factors) that are defined following a specific expression [17, 31].

Due to the requirement of the URQ technique to evaluate the objective functions at a specific point, the R.R.E.A. can be used for systems that require the analysis of interest to be performed under any conditions. The advantage of being able to approximate the statistical quantities by evaluating the objective function only $2n + 1$ times, an attractive quality for a computationally expensive system, can be exploited if the analysis does not get stuck for some reason at one of the $2n + 1$ analyzed conditions.

As previously stated, the optimization is based on the self-adaptive differential evolutionary paradigms. All Differential Evolutionary algorithms comprise of three main steps that need to be followed after having generated the first population: mutation, crossover and selection. The adopted DE algorithm is the self-adaptive one proposed in [25] but with the addition of these steps in the process. The additional steps are as follows (see flow diagram in Figure 4):

- reduction in the dimension of the population. This step is considered when the 'if-conditions' are fulfilled. Labeling $N_{max_{Feval}}$, p_{max}, NP and $count_G$ as the maximum acceptable number of function evaluations, maximum number of population size reduction, population size and

number of evaluated generations, the mathematical expression of such a condition is

$$count_G > \frac{N_{max_{Feval}}}{p_{max} \cdot NP} \tag{7}$$

The meaning is that considering the worst case scenario, the number of populations evaluated for all the possible reduced generations needs to be less than the maximum number of function evaluations. The condition presented in equation (7) on one hand is conservative since it considers that actually all the possible p_{max} reductions will be done and it does not take into account that the current population size NP can be reduced; on the other hand it does not consider that NP could have been greater in previous steps.

- stratagem to avoid local minimum. This step has been introduced in order to avoid that a local optimum, determined after a certain number of evaluated generations $count_G$, can 'monopolise' the optimization process. To this end, a random variation of the identified best individual is generated.

- sorting the individuals at the end of the algorithm depending on the relative values of the objective function. At the end of the optimization process, it has been considered necessary to sort the set of obtained values for the quantity of interest and relative input factors in order to keep the best ones at the beginning of the ordered set of quantities. Such a sorting is significant if then a reduction of the size of the population is considered and some individuals of the population in the previous generation are excluded from the iterative process.

The selected stopping criterion is in terms of the maximum number of generations G_{max} and/or the error with respect to the desired optimum value of the objective function $VTR \pm \epsilon$, if known or given.

In order to use the presented evolutionary algorithm some constants need to be fixed, thus the goodness of the results depends also on these values. The constants are τ_F,τ_{CR},p_{max}, NP_{min}, NP_{init}, $N_{max_{Feval}}$, VTR, ϵ, G_{max},F_{upp}, F_{low}, CR_{upp}, CR_{low} and are defined depending on the analyzed problem.

Validation of the enhanced jDE algorithm The enhanced self-adaptive differential evolutionary algorithm has first been verified by performing the minimization of functions that are commonly

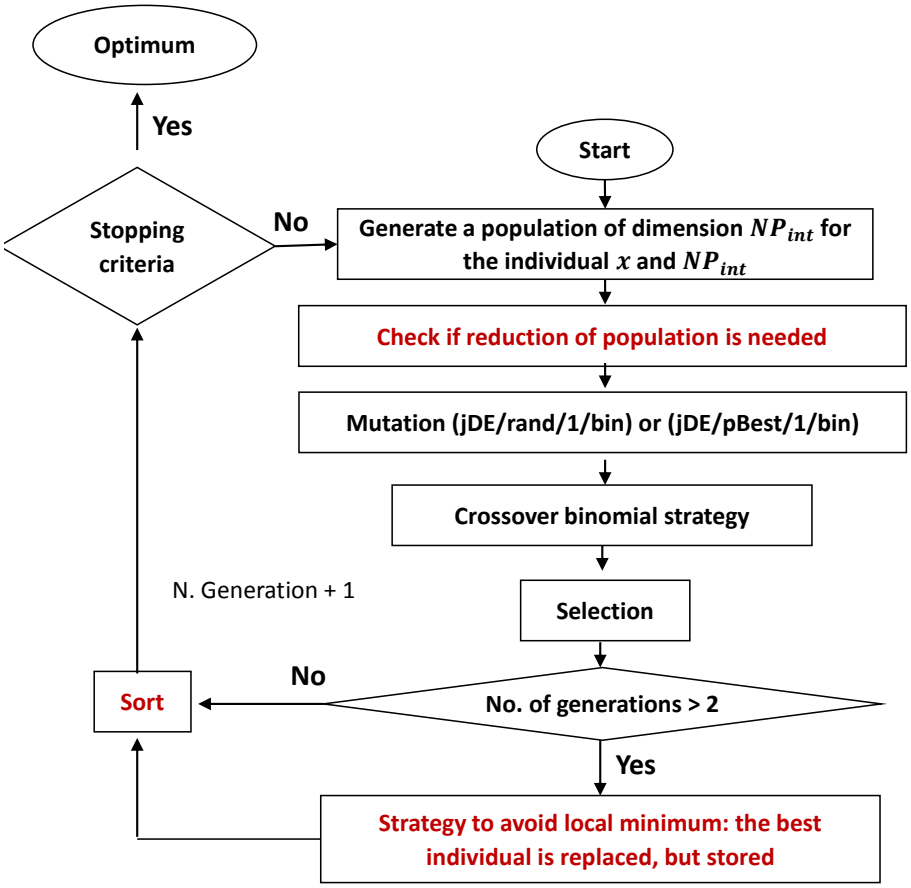

Fig. 4: Flow chart describing the iterative phase of the R.R.E.A..

used to test optimization algorithms [33]. In almost all cases, the number of generations needed to converge to the global optimum of the function if the original jDE is used decreases if the enhanced differential algorithm is adopted. Moreover, some of the considered functions (Rosenbrock10, Griewank and Sphere10) do not converge even with 10000 generations when the old algorithm is adopted. For further information, see [34].

III. Case study and bifurcation analysis

The validation considers the occurrence of shimmy phenomena in landing gear systems during ground manoeuvres [29, 35, 36]. Shimmy results from the nonlinear interaction between the follower forces acting on the tyre and the modes of vibration, resulting in Limit Cycle Oscillations (LCOs). Bifurcation analysis serves as an efficient methodology to determine the boundaries of stable dynamic regimes [37, 38].

The implementation of bifurcation analysis entails the solution of all the steady states of the system in the parameter range of interest, along with a determination of their stability. Changes in local stability as a parameter varies are then assessed using bifurcation theory to infer the mechanisms governing more global behavior.

The results obtained performing bifurcation analyses can be graphically visualized and the plots are called bifurcation diagrams. Various methods can be adopted to perform bifurcation analysis, identifying the equilibrium branches for bifurcation diagrams and bifurcation points, possibly also evaluating the *periodical solutions* in more than one parameter. Continuation analysis has been adopted here since it gives the possibility of analyzing both equilibrium and periodical solutions and of performing bifurcation analysis directly using multi-body systems. Considering numerical continuation, it is first necessary to define the set of parameters to be varied in order to investigate possible changes in stability of equilibrium solutions; these parameters are called bifurcation parameters. Then equilibrium solutions need to be determined in terms of the variation of one of the selected bifurcation parameters, detecting the occurrence of possible bifurcation points such as Hopf bifurcations (HB). A Hopf bifurcation typically occurs when a complex conjugate pair of eigenvalues of the linearised system at a fixed point becomes purely imaginary; thus this kind of bifurcation can only occur in systems of dimension two or higher. In the presence of such critical points, the locus of bifurcation points can be investigated as more than one parameter changes, and shown on two-parameter bifurcation diagrams. Moreover, if the bifurcation point is an Hopf bifurcation, then limit cycle oscillations occur and the maximum amplitude and period characterizing the relative periodic response of the system can be determined.

Considering *shimmy* in the landing gear as the case study, the selected bifurcation parameters are the forward velocity V and the vertical load along the main structure of the landing gear. The reason for this choice is the considerable variation of these parameters during landing and take-off manoeuvres:

- the variation of the vertical load is strictly related to the loading condition (for instance lift relative to weight during take-off, landing or taxing). In the present paper, an upper force limit of $4 \cdot 10^5$ N is considered.

- the forward velocity V during a landing manoeuvre must fulfil regulatory certification requirement; tables provided in an International Civil Aviation Organization (ICAO) document ([39]) indicate the range of handling speeds for each category of aircraft to perform the manoeuvres specified. These speed ranges are assumed for use in calculating airspace and obstacle clearance requirements for each procedure. Taking into account the information provided by ICAO, the range of interest for the forward velocity V is taken as $[0-100\text{m/s}]$ in the analysis.

Moreover, the aim of the analysis is to investigate the variation of occurrence of Hopf bifurcation points in the operational parameter space usually considered for ground manoeuvre, i.e. in the (vertical load, forward velocity) space. Having defined the vertical load and the forward velocity as bifurcation parameters, the variation of locus of Hopf bifurcation points in the defined operational parameter space can be investigated as other parameters change.

Figure 5 shows deterministic bifurcation diagrams in terms of one bifurcation parameter (the forward velocity V) and maximum amplitude of the torsional state ψ for the periodic solution (LCO) for a landing gear model ; Figure 6 is an associated two-parameter bifurcation diagram, in particular shows the locus of Hopf bifurcation in a 2 dimensional space idenitfied by the forward velocity V and the vertical load F_z, i.e. the set of points (V, F_z) for which Hopf bifurcation occurs.

The analysis has been performed using AUTO as the continuation and bifurcation software ([40]). Since the developed methodologies are implemented in Matlab, the Matlab version of AUTO (the Dynamical System toolbox [41]) has been adopted. The Dynamical System toolbox integrates AUTO into Matlab via mex functions to perform bifurcation analysis of dynamical systems for which an analytic description is available or that are modelled in software able to interface with Matlab.

A. Landing Gear Model

The landing gear model is analytic and is taken from Howcroft ([42]). It represents a dual-wheel landing gear in which free-play and wheel gyroscopic effects are omitted. The deflection of the landing gear structure is modeled in terms of three degrees of freedom (Figure 7) and an additional DoF is introduced for the tyre dynamics. There are seven states, since the equations for

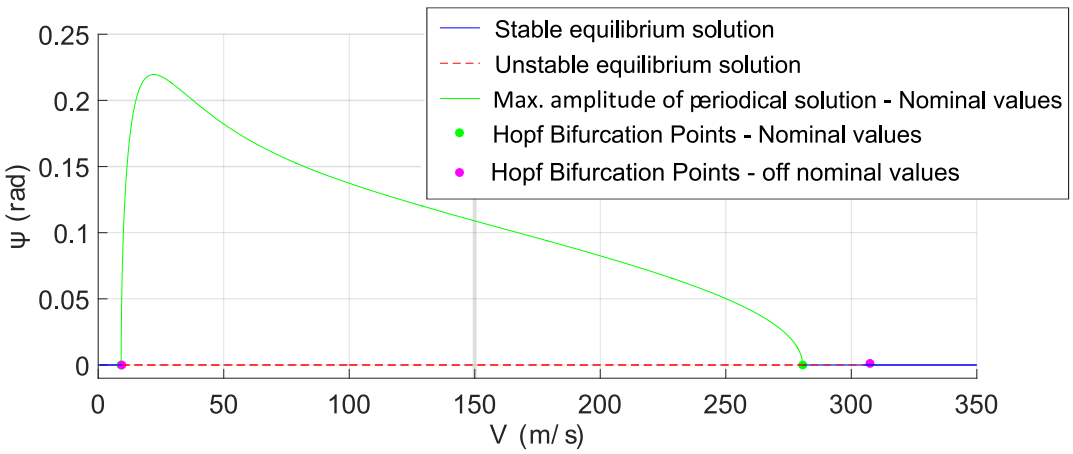

Fig. 5: Deterministic bifurcation diagrams in one parameter, the forward velocity V, with periodic branches.

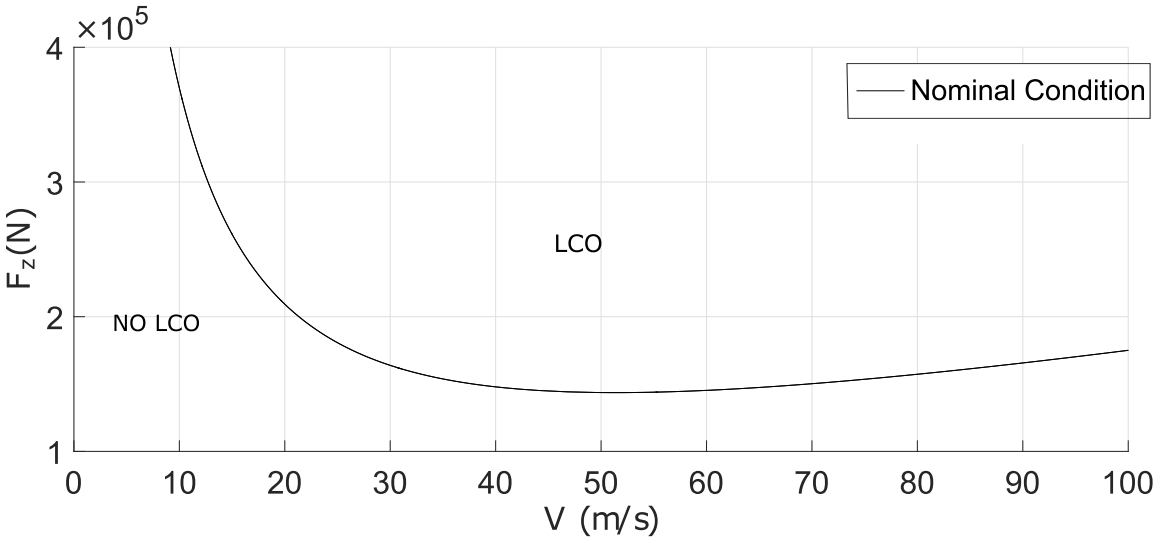

Fig. 6: Deterministic bifurcation diagrams in two parameters, the forward velocity V and the vertical load F_z.

the first three DoFs are of second order while the last is of first order. The degrees of freedom are:

1. torsional, ψ, describing the rotation of the wheel/axle assembly about the local axis z;
2. in-plane, δ, expressing the bending of the oleo piston in the side-stay plane. This DoF is approximated as a rotation about a point at a distance L_δ from the axle;
3. out-of-plane, β, describing the rotation of the landing gear about the two attachment points;

4. lateral tyre displacement, λ, as defined for the straight tangent model ([43]).

The first three DoFs above-mentioned are clarified in figure 7 considering a zero rake angle ϕ.

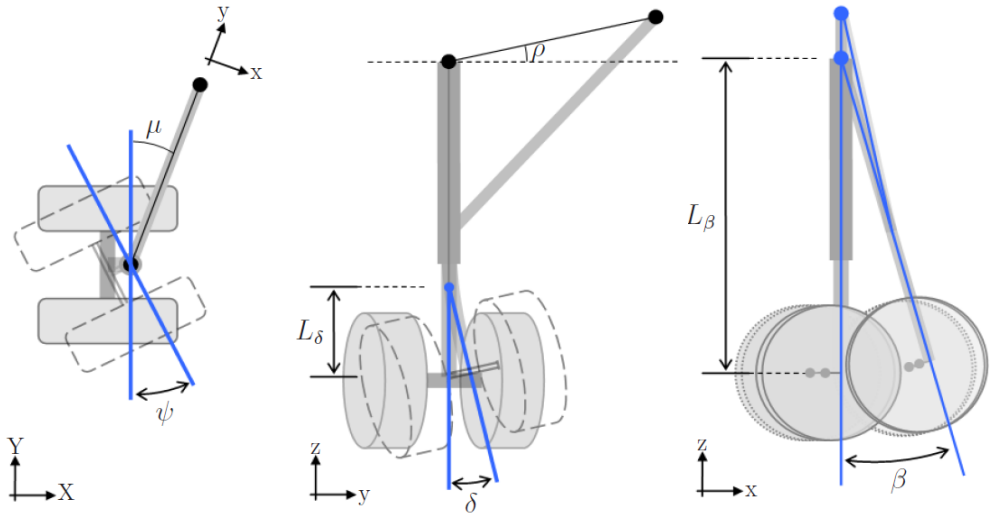

Fig. 7: DoFs characterising the adopted landing gear model ([42]). (XYZ) and (xyz) are the global and local coordinate systems.

Further details on the landing gear model can be found in [29], where it was used to perform uncertainty quantification in terms of shimmy phenomena. In the following section the results obtained using both the I.D.E.A. and R.R.E.A. algorithms are presented.

IV. Application and Results

The application of the optimization techniques presented in section II has the aim of optimizing the landing gear design whilst decreasing the probability of occurrence of shimmy during ground manoeuvre. Figure 8 shows an example of what can occur due to uncertainty in the system.

The continuous blue and red lines are the lower and upper confidence bounds for the loci of Hopf bifurcation points determined using the SVD based method ([19, 29, 30]). The dashed red line is the operational trend, defined later. For all the values of the forward velocity V between the first and second intersecting points, LCO (shimmy) can occur due to the uncertainty in the system.

The I.D.E.A. technique has the aim of decreasing the probability of occurrence of shimmy during ground manouevres. In particular, this has been addressed here by making the probability

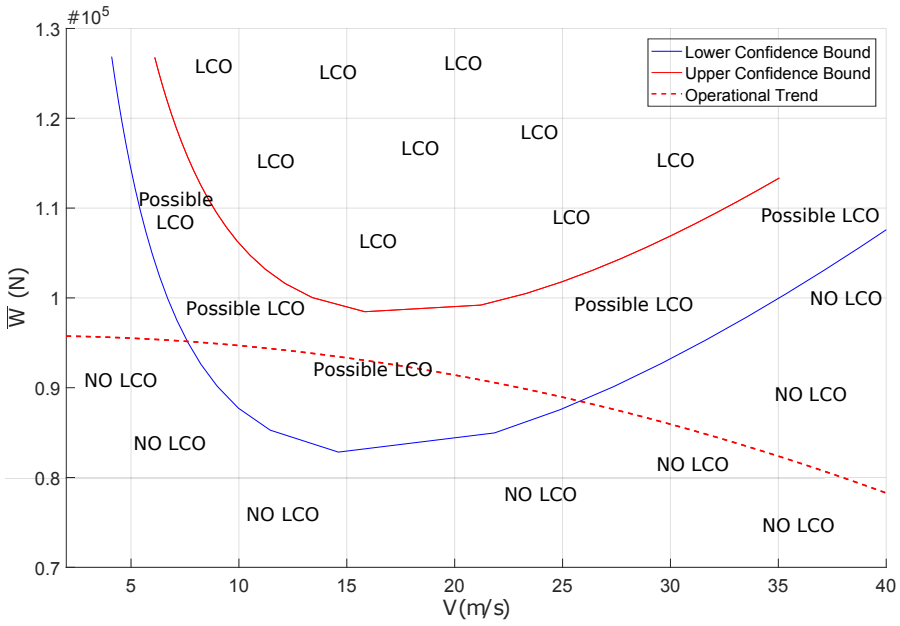

Fig. 8: Example of lower and upper confidence bounds for the loci of Hopf bifurcation points and operational trend.

of intersection between the loci of interest (loci of Hopf bifurcation) and the limit state function (the operational trend) as low as possible.

The R.R.E.A. technique minimizes one of the three selected objective functions (Case 1: $f(\mathbf{x}) = \mu_d + S\sigma_d$, Case 2: $f(\mathbf{x}) = |\mu_d + 4\sigma_d|$, Case 3: $f(\mathbf{x}) = \sigma_d$) considering as the function of interest $d(\mathbf{x})$ the distance of the point on the locus of Hopf bifurcation that is at the maximum positive distance from the point on the same direction of interest but on the limit state function. It can be expressed as

$$\sqrt{(\overline{W}_{operational} - \overline{W}_{loci})^2 + (V_{operational} - V_{loci})^2} \tag{8}$$

where $\overline{W}$ stands for the generic vertical load, and the subscripts *operational* and *loci* are adopted to indicate if the considered point is on the operational trend or on the locus of Hopf bifurcation.

The direction of interest for which the stated distance is maximum, is called critical. Figure 9 shows the mean and deviation considered to define the objective functions along the critical direction of interest and assuming a symmetric distribution for an exemplar function (the red line is

the point on the operational trend intersecting the critical direction of interest). It is apparent that the selected objective function is chosen such that the mean is negative, i.e. the point on the critical direction corresponding to the mean is not inside the region where LCOs occur (which is limited by the operational trend), and the minimization of the mean is actually giving a maximization of the distance of the locus of Hopf bifurcation point from the operational trend.

The three considered cases for the optimization are now explained.

Case 1 evaluates the distance along the critical direction of the tail of the PDF of f at a point identified by the value assumed by the variance, thus assuring reliability and determining a conservative result since it can be far from a simple tangency between the lower bound of the locus of Hopf bifurcation and the operational trend.

Case 2 looks for the parameter values that gives the tangency assuming that the tail ends at $4\sigma_d$.

Case 3 requires more robustness, minimizing the variance, and the system might not be sufficiently reliable, i.e. intersection between the lower bound and the operational trend can occur. For Case 3, two situations are analysed, i.e. including or excluding a constraint on the mean μ_d during the optimization process. The constraint requires that the optimum is characterized by a negative mean; the optimization code discharges the solutions for which μ_d is greater than 0, i.e. the locus of Hopf bifurcation is certainly intersecting the operational trend. In fact, μ_d is the mean of the distance function d that is always negative in the absence of intersection.

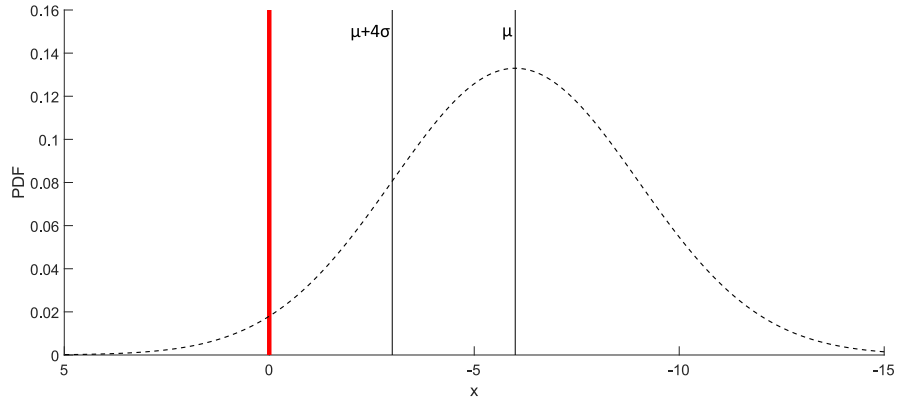

Fig. 9: Mean and deviation considered to define the objective functions adopted in R.R.E.A. .

The second optimization process (R.R.E.A.) can be used for systems that allow the analysis of interest to be conducted at any conditions: URQ (section II C) has been adopted to compute statistical quantities of the output of interest, which requires $2n+1$ evaluation of the responses of interest (significantly less computational expensive than MCS). This aspect is important if bifurcation analysis is adopted. In fact, it would be unfeasible to determine statistical quantities without the use of techniques based on the evaluation of a significantly smaller number of bifurcation diagrams than the one required by techniques such as MCS. This constraint is due to the computational burden of bifurcation analysis applied to the landing gear system; for instance the indicative times required to compute the bifurcation diagram in 1 and 2 parameters are 12 and 52 seconds, respectevely.

Here, the phases characterizing the developed methods are followed and discussed step by step.

A first element that is common to both the I.D.E.A. and R.R.E.A. approach is the definition of the limit state function g. This is the variation of the vertical load on the landing gear as the forward velocity changes during a static manoeuvre on the ground of an illustrative aircraft in equilibrium conditions. The stated variation can be defined by employing equilibrium equations. The explicit expression of the stated variation is given by

$$F_n = \frac{B_m}{B}(W - L) \qquad L = \frac{1}{2}\rho V^2 S C_L \tag{9}$$

where B_m is the track of the main assembly, B is the distance between the nose and the axis of the main assembly, W is the weight of the aircraft, ρ is the air density, S is the equivalent surface and L is the lift (Figure 10).

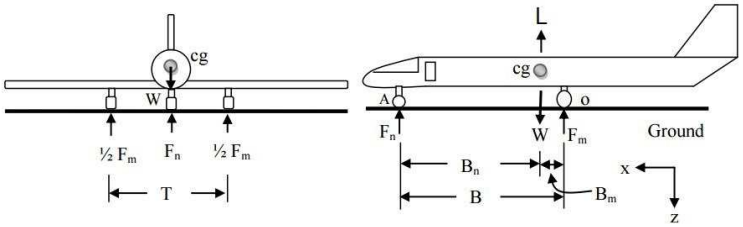

Fig. 10: Aircraft free body diagram.

Another common element is related to the interval of variation, the tolerances adopted in the I.D.E.A. and all the coefficients that need to be defined in the Evolutionary Algorithm (Table 1).

Variable	Value
$P_{max_{i_{low}}} = P_{max_{i_{upp}}}$	P_{max}
Tol_ϵ	0.01
Tol_p	0.05
$N_{max_{Feval}}$	value sufficiently high so as not to prematurely stop the iterative optimization process
τ_F	0.01
τ_{CR}	0.01
ϵ	10^{-5}
VTR	10^{-5}
N	3, dimension of the uncertain factors
F_{upp}	1
F_{low}	0.2
CR_{upp}	1
CR_{low}	0.05
NP_{min}	3
NP_{init}	10
G_{max}	$30 \cdot log(2 \cdot D)$
min_x, max_x	are the last coefficients to be set depending on range of variation for the parameters

Table 1: Values considered for the coefficients used in the optimization.

The values adopted for τ_F and τ_{CR}, ϵ and VTR, $F_{upp}, F_{low}, CR_{upp}$ and CR_{low} and p_{max} are kept equal to those identified as appropriate during the validation performed on the objective functions stated in subsection II C. The values adopted for the minimum and initial population size (NP_{min} and NP_{init}) are to assure a combination of generations at an acceptable computational time. The same considerations have been made to select the value for the maximum number of generation G_{max}. However, more investigation into the computational burden and accuracy of the solution can be carried out, if of interest, changing the selected values for the parameters.

Latin Hypercube Sampling (LHS) is the technique adopted to define the sampling planes for initializing the design/uncertain factors and the parameters in the mutation and crossover steps (F and CR).

In what follows, the results obtained applying I.D.E.A. and R.R.E.A. to the landing gear are presented.

For both techniques, first of all the values adopted to define the limit function trend are specified (Table 2). Then, the variables and the percentage variation need to be defined. The variables for the analytic model are selected as those that most influence the most the problem of interest, which have been determined in a previous investigation by the authors ([19]): the damping and the moment of inertia for the torsional degree of freedom (c_ψ, I_ψ) and the tyre relaxation length L. Two choices of percentage variation of these variables are considered for the I.D.E.A. technique: P_{max} fixed equal to 3.5% (Example 1) and 7% (Example 2). Only the first of these ($P_{max} = 3.5\%$), is applied if the R.R.E.A. technique is considered. Adopting the surrogate models trained using the bifurcation diagrams already evaluated to perform the Uncertainty Quantification in a previous work ([19]), the set of values $\mathbf{F}_G^*$ and the interval (eq. 5) have been determined for each considered case. From this point, different approaches need to be followed depending on the adopted strategy. First the I.D.E.A. and then the R.R.E.A. strategies and results are presented.

parameter	value
B	11.04 m
x_{cg}	8.6m
B_m	$Bm = B - x_{cg}$
W	$8 \cdot 10^4$ kg
ρ	1.225kg/m^3
$S \cdot C_L$	128.1m^2

Table 2: Values adopted to describe the limit function for the optimization of the analytic landing gear design.

I.D.E.A. Considering the I.D.E.A. strategy, the evolutionary phase starts and Fig. 11-15 provide the results obtained for the first of the two considered examples (i.e. $P_{max} = 3.5\%$) for one generation each, where the green point stands for $\mathbf{F}_G^*$. The hypercubes in the parameter space (in this case a cube) are determined and sorted in an ascending order. Using a full factorial design, the

hypercubes are filled with points (red in Fig. 12) and the QoI (F_n and V) are evaluated for the points inside the initial range of variation for which the surrogate models are trained. The dimension of such a full factorial design is 36. Negative points, i.e. those for which the locus of Hopf bifurcation points intersect with the operational trend under the considered tolerance, are determined (yellow points in Fig. 13) and the hypercube is further subdivided as explained in section II B. At this step, AUTO is run for all the other sampling points inside the hypercubes that can be further considered due to containing the point $\mathbf{F}_G^*$ and no negative points. Finally, the hypercubes are sorted again and the one with the greatest volume is picked out for each considered generation and the optimum sets are determined (Fig. 14). A post-processing of the data can be considered and the SVD (Singular Value Decomposition) based method can be applied to eventually propagate the uncertainty for the determined optimum sets (the black points in Fig. 15).

The comparison of the initial confidence bounds and the optimum ones are shown in Fig. 16 and 17 for Example 1 and Example 2, respectively. Moreover, Fig. 18 shows a comparison of the loci of quantiles for the initial and optimum confidence bounds obtained for Example 2.

Finally, for the sake of completeness Fig. 19 shows a comparison of the PDFs obtained for the initial set of nominal values and the optimum set, considering the same percentage of variation (3.5% and 7% for Example 1 and Example 2, respectively). Table 3 provides the initial set of nominal/percentage values and the optimum set and relative acceptable uncertainties.

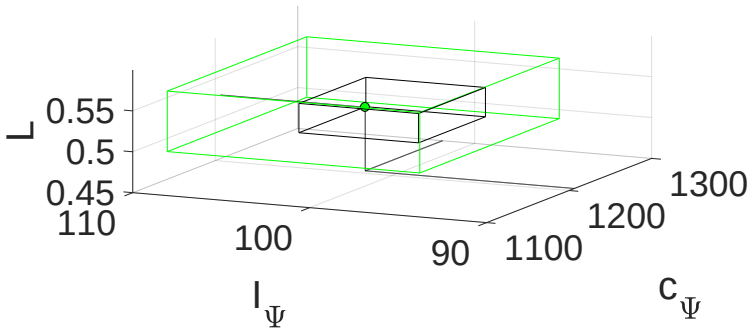

Fig. 11: I.D.E.A. - one generation step. The green point is related to the locus of interest tangent to the limit-state function.

Using the identified optimum set of values, the probability of failure related to the points on the

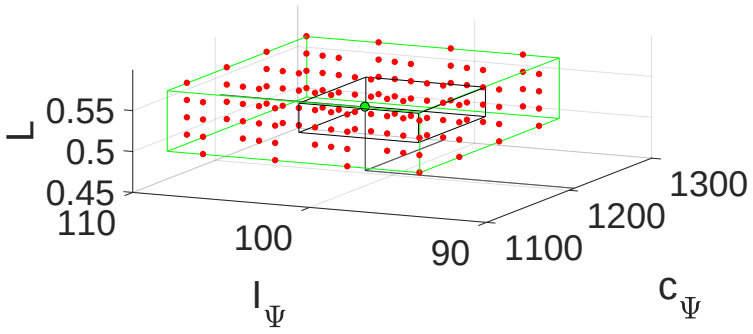

Fig. 12: I.D.E.A. - Full factorial design.

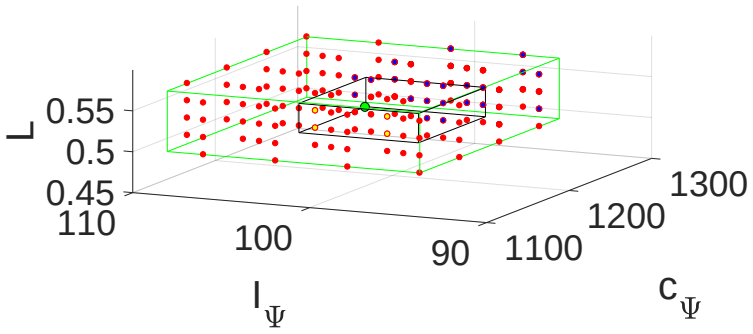

Fig. 13: I.D.E.A. - Mutation step. The yellow points are the negative ones.

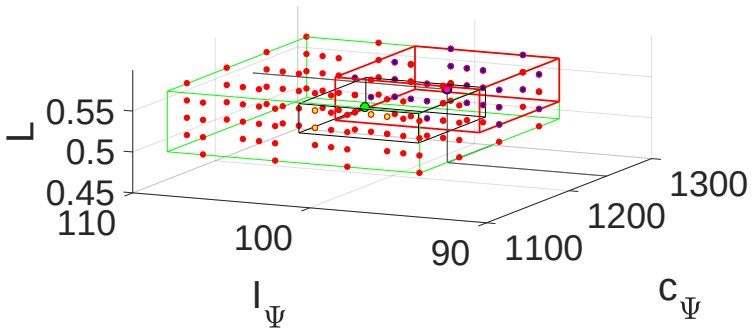

Fig. 14: I.D.E.A. - Mutation step and selection of the best hypercube (in red). The selected optimum set of parameters is the magenta point.

locus of Hopf bifurcation determined for the starting landing gear design, intersecting the direction of interest and belonging to the region of failure, are shown in Table 4. The stated points of interest inside the region of failure are two and three for the Example 1 and Example 2.

The results show a very encouraging achievement for the proposed novel optimization algorithm

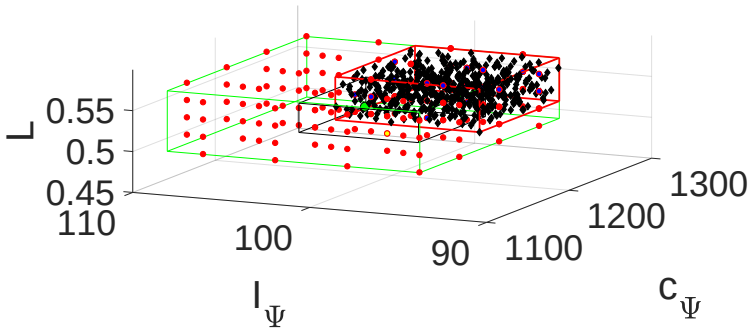

Fig. 15: I.D.E.A. - Optional postprocessing analysis. The loci are evaluated using the SVD based method at the black points.

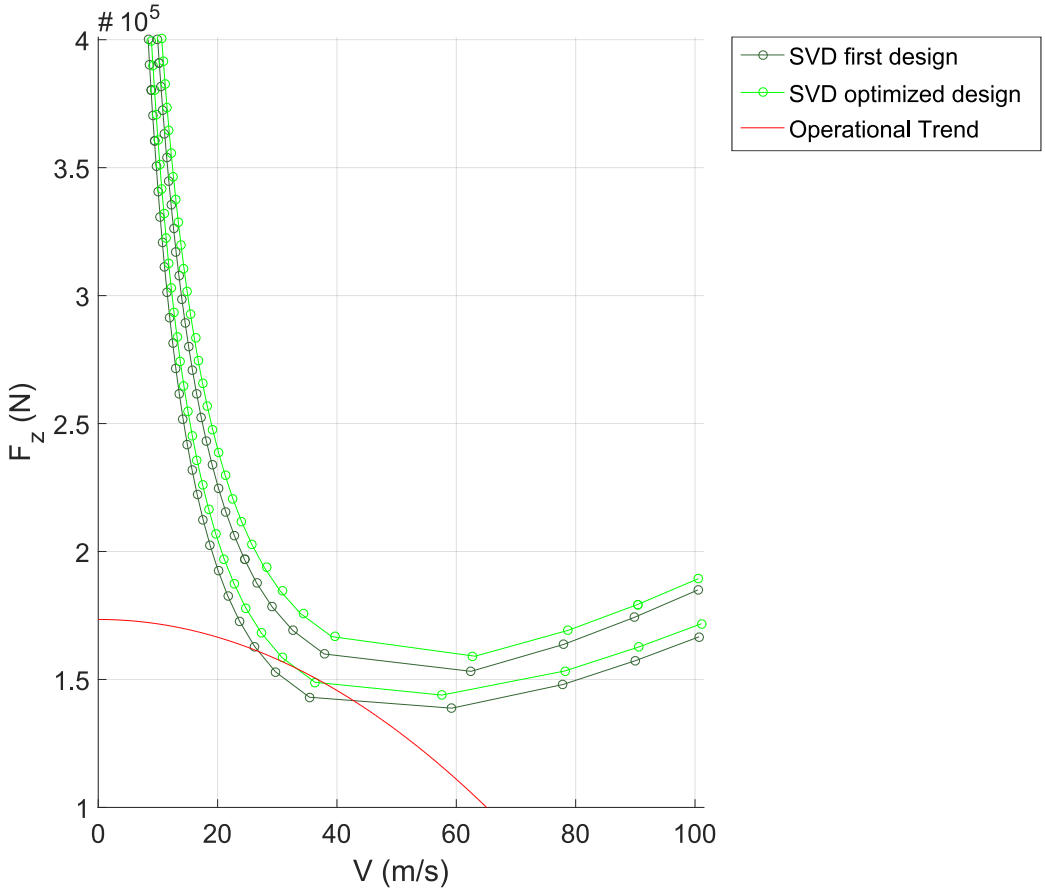

Fig. 16: Comparison of the initial confidence bounds and the optimum bounds for Example 1.

(I.D.E.A). The lower confidence bound of the loci of Hopf bifurcation moved, decreasing the probability of failure and assuring a reliable structure. Moreover, a high level of robustness is retained,

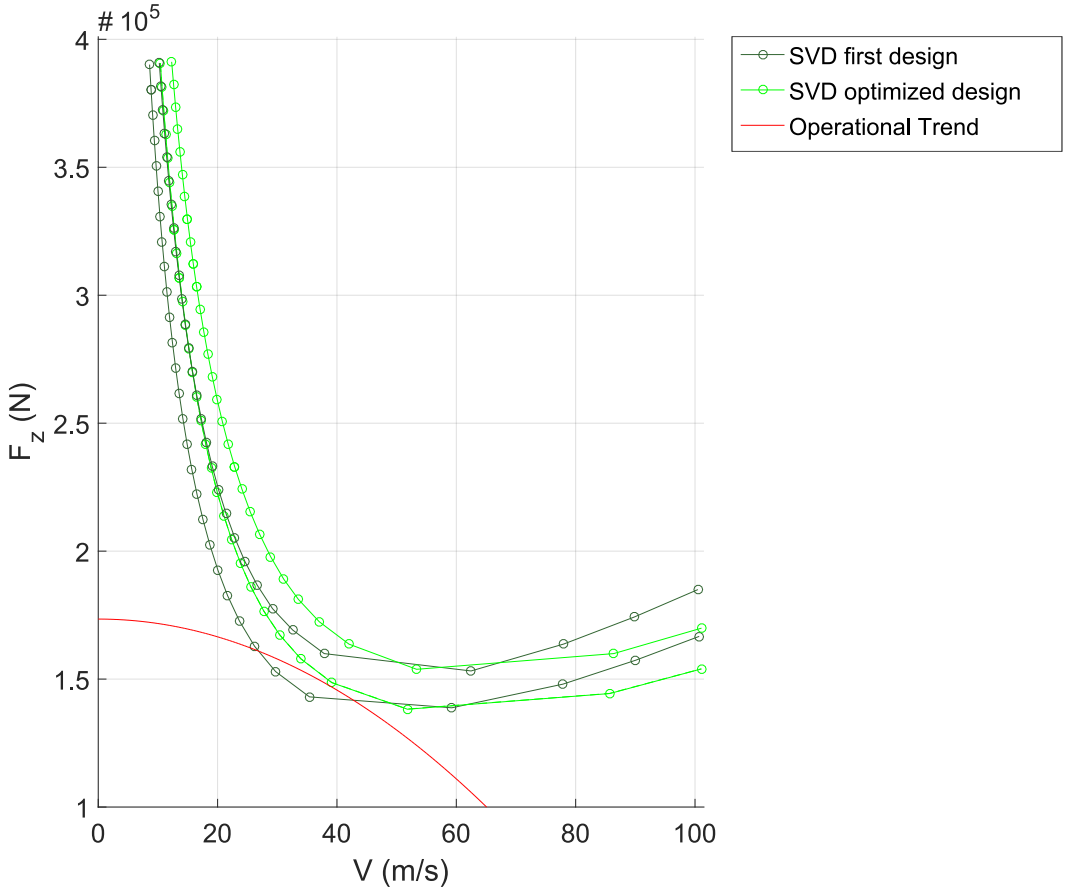

Fig. 17: Comparison of the initial confidence bounds and the optimum bounds for Example 2.

	Example 1	Example 2
	$[c_\psi, I_\psi, L]$	$[c_\psi, I_\psi, L]$
Starting Point	$[1200, 100, 0.53]$	$[1200, 100, 0.53]$
Optimum	$[1189.80, 91.72, 0.525]$	$[1217.404, 90.6, 0.579]$
Initial Uncertainty Range (%)	$[3.5, 3.5, 3.5]$	$[7, 7, 7]$
Acceptable Uncertainty (%)	$[4.56, 4.77, 4.56]$	$[8.27, 7.48, 10.09]$

Table 3: Results obtained applying I.D.E.A. to the analytic landing gear model considering two different sets of uncertainties.

which is shown by the width of the PDF along each direction of interest starting from the points on the discretised locus of Hopf bifurcation that are between the intersections with the operational

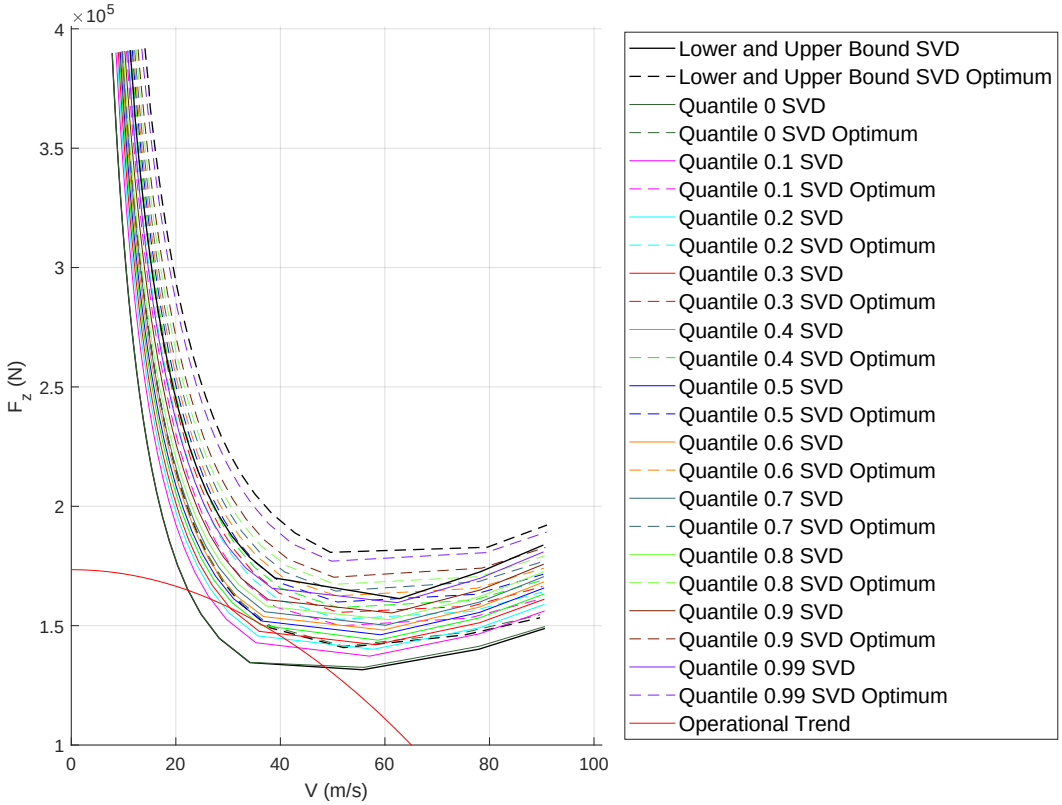

Fig. 18: Comparison of the loci of quantiles for the initial and optimum confidence bounds obtained for Example 2.

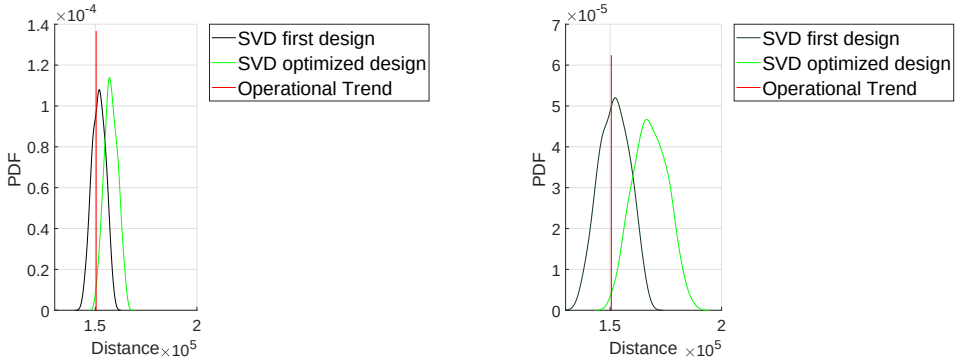

(a) 3.5% variation, Example 1

(b) 7% variation, Example 2

Fig. 19: Comparison of PDF obtained for the initial set of nominal values and the optimum one.

trend. Finally, thanks to the introduced iterative procedure, there is no requirement to perform bifurcation analyses and then give statistical properties to the results, propagating the uncertainty.

	Example 1		Example 2		
Direction of Interest	1	2	1	2	3
SVD					
Starting Design	$1.294 \cdot 10^{-1}$	$3.715 \cdot 10^{-1}$	0.1063	$3.326 \cdot 10^{-1}$	$4.68 \cdot 10^{-1}$
Optimized Design	$3.0372 \cdot 10^{-4}$	$1.99 \cdot 10^{-2}$	$4.9 \cdot 10^{-4}$	$9.7 \cdot 10^{-4}$	$7.5 \cdot 10^{-3}$

Table 4: Probability of failure for the starting design and for the best optimum landing gear design.

In the presented method the uncertainty is considered throughout the optimization procedure and there is no need to propagate them separately for each set of design parameters.

R.R.E.A. If the R.R.E.A. technique is adopted, after having selected the range of variation for the input parameters selected in the optimization process, the enhanced evolutionary algorithm presented in section II C can be applied. The range of variation considered for the nominal values of the three more influential parameters is presented in Table 5. Moreover, since the URQ is adopted then the first four statistical moments of the input factors need to be specified. The first statistical moment, the mean, is fixed to the values characterizing each individual in the populations used in the evolutionary algorithm. The other statistical quantities are determined assuming a continuous uniform distribution for the design factors, i.e.

$$\sigma^2 = \sqrt{(max(x_{iG}) - min(x_{iG}))^2/12}); \qquad \gamma = 0; \qquad \Gamma = -6/5 + 3; \tag{10}$$

where i and G are the indexes adopted for the individual of the population and the generation at which the population belongs, respectively.

Parameter	Label	Maximum	Minimum
inertia of ψ DoF	I_ψ	105.01	91.29
damping coefficient of ψ DoF	c_ψ	1262.13	1097.18
tyre relaxation length	L	0.566	0.492

Table 5: Parameters and the range of values adopted in the optimization using R.R.E.A. technique.

The investigation has been carried out considering the three defined objective functions (case 1: $f(\mathbf{x}) = \mu_d + S\sigma_d$, case 2: $f(\mathbf{x}) = |\mu_d + S\sigma_d|$, case 3: $f(\mathbf{x}) = \sigma_d$). Five different values for the coefficient S have been adopted.

MCS with 100 sampling points is used for the validation of the approximated statistical quantities. Table 6 shows the obtained results for the nominal case, i.e. adopting the mean values for I_ψ, c_ψ and L, and for the optimized cases.

The results from the validation reveal that sometimes the discrepancy between URQ and MCS approximations can reach 28%. The error can be due to one or the other approximation: the only conclusion that can be made is that there is a lack of coherence between the two approximation methods. Looking at the mean and deviation, and making a comparison with the one related to the nominal conditions, it is apparent that minimizing the objective function, and so the distance of the point on the PDF along the critical direction of interest from the limit state function (the operational trend), the results are always reliable but the robustness is higher if the coefficient S is higher. In fact, the reliability is assured by the selected objective function while the robustness is linked to the obtained variance. As stated in section II C, the general expectation is that the greater the coefficient S the more the variance should be minimized and the results obtained for case 1 confirm such a statement (Table 6). In fact, this cannot in general be assured since mathematically it can also happen that having increased the coefficient S, the required minimization is reached for a decreasing of the mean that does not require the variance to decrease more than that related to a higher value of S.

For the sake of conciseness, only the probability distribution along the direction of interest for each case is here shown (Figures 20 - 22). The probability of failure is zero for all the considered cases with the only exception of Case 3. In Case 3 the probability of failure along all the critical directions of interest is equal to 1 if the constraint on the mean is not taken into consideration, otherwise the maximum probability of failure on the stated direction is reduced relative to the nominal case (Figure 22). In fact, in the nominal case the probability of failure along such a direction is 0.4 and after the optimization considering Case 3, with the constraint, it is 0.1.

Considering the results presented here it is apparent that these is significant potential for using

case	$\mu_{f_{MCS}}$	$\mu_{f_{UQR}}$	$\lvert\epsilon_\mu\rvert$	$\sigma^2_{f_{MCS}}$	$\sigma^2_{f_{UQR}}$	$\lvert\epsilon_\sigma\rvert$
Nominal	-860.35	-623.58	0.83	3433.5	3404.9	27.52
case 1: $S = 1$	-34370.5	-35099.7	2.12	6253.7	6481.3	3.64
case 1: $S = 3$	-43335.24	-44057.87	1.67	5971.92	4395.49	26.4
case 1: $S = 5$	-34629	-34266.8	1.05	3996.24	4034.64	0.96
case 2: $S = 4$	-14305.73	-13901.27	1.23	3491.83	3448.87	2.83
case 2: $S = 8$	-29457.4	-29551.6	0.32	3741.72	3883.1	3.78
case 3: no mean	11693.14	11680.14	0.11	3144.47	2789.09	11.3
case 3: mean	-4091.64	-4417.23	7.96	3257.48	4200	29

Table 6: Results obtained applying R.R.E.A. to the analytic landing gear model for three different objective functions.

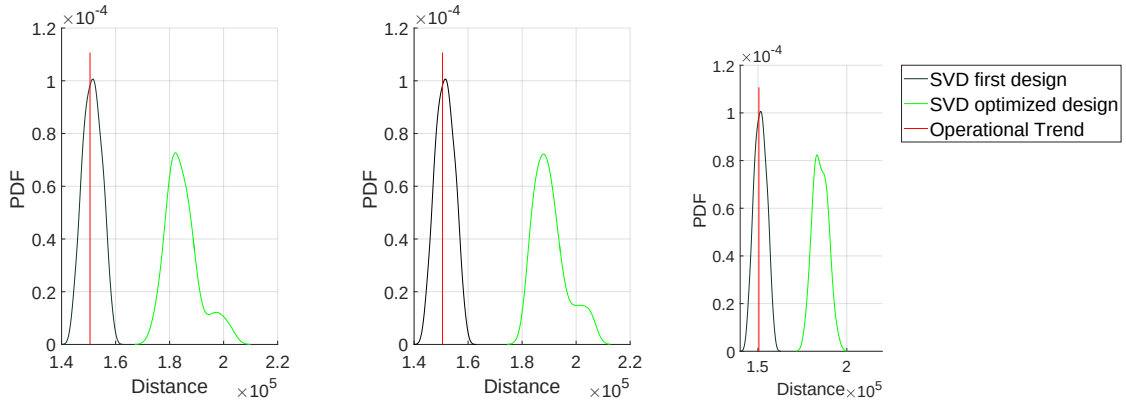

(a) $S = 1$ (b) $S = 3$ (c) $S = 5$

Fig. 20: PDF obtained considering case 1 for the objective function.

the enhanced differential evolutionary algorithm together with Univariate Reduced Quadrature for complex analyses that assure acceptable results to be achieved whatever condition in the acceptable range of parameter variation is considered. This approach has been demonstrated using three different objective functions: in all three cases the expectation is completely met. In Case 1 the variance decreases as the weight factor S increases; in Case 2 the tangency between the lower bound and the operational trend is obtained as desired. It can be observed that the variation of S in this case does not significantly influence the final results. In Case 3 the variance is minimized and it has

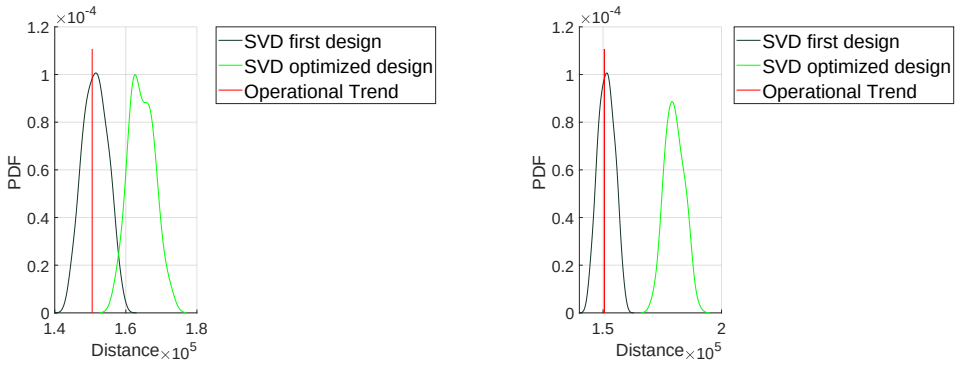

(a) $S = 4$ (b) $S = 8$

Fig. 21: PDF obtained considering case 2 for the objective function.

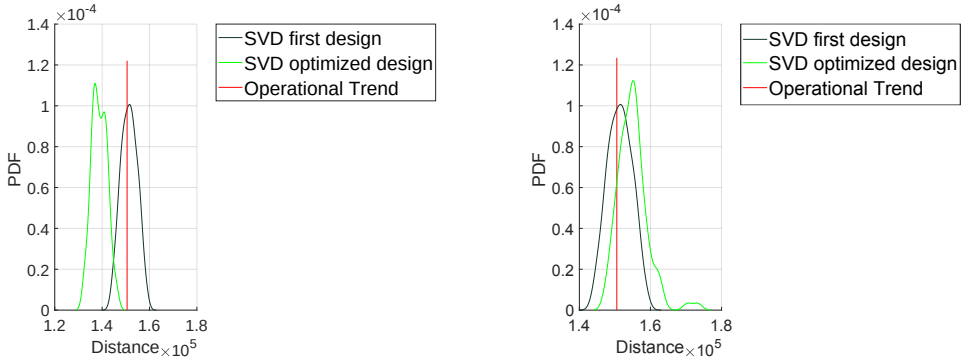

(a) Without constraints on the mean. (b) With constraints on the mean.

Fig. 22: PDF obtained considering case 3 for the objective function.

been proved that the constraint on the mean μ_d must be considered in order to obtain an acceptable probability of failure.

V. Conclusions

The Iterative Distribution Evolutionary Algorithm and Reliable & Robust Evolutionary Algorithm optimisation strategies were shown to be capable of dealing with objective functions that are related to expensive nonlinear analyses and involve correlated quantities. The application of both the iterative differential evolutionary and the reliable and robust evolutionary algorithm in minimizing the probability of onset of shimmy for a landing gear system during ground manoeuvre has given encouraging results. The techniques have been able to limit the number of evaluations of the objective function, to guarantee a minimization of the probability of failure while limiting

approximations in evaluating the objective functions of interest, to identify the maximum range of parameter variation for the investigation and to avoid gradient calculations. Adopting I.D.E.A. enables reliable results to be obtained, while R.R.E.A. gives the possibility of investigating reliable and/or robust solutions. Finally, the comparison that was performed between the enhanced (in R.R.E.A.) and the standard (jDE) differential evolutionary algorithms, using commonly applied optimization test functions, confirmed the improved efficiency of the proposed approach. Since the obtained promising results, a further work would be to validate and compare the developed methods with performance of other techniques in order to justify adoption of the algorithms in practice.

Acknowledgment

This work was supported by the European Commission (EC FP7) under the Marie Curie European Industrial Doctorate Training Network 'ALPES' (Aircraft Loads Prediction using Enhanced Simulation) and also the Royal Academy of Engineering.

References

[1] Choi, S. K., Grandhi, R. V., and Canfield, R. A., *Reliability-based Structural Design*. Springer-Verlag London Limited, 2010. DOI: 10.1007/978-1-84628-445-8.

[2] Zeljković V. and Maksimović, S., *Multilevel Optimization Approach Applied to Aircraft Nose Landing Gear*. Scientific-Technical Review, Vol.LVI, No.2, 2006.

[3] Mastroddi, F. and Gemma, S., *Analysis of Pareto frontiers for multidisciplinary design optimization of aircraft*. Aerospace Science and Technology, July 2013, Vol. 28, No.1, pp. 40âĂŞ55. FOI: 10.1016/j.ast.2012.10.003

[4] Swati, R. F. and Khan, A. A., *Design and Structural Analysis of Weight Optimized Main Landing Gears for UAV under Impact Loading*. Journal of Space Technology Vol.4, No.1, July, 2014.

[5] Swati, R. F. and Khan, A. A., *Design and Structural Analysis of Weight Optimized Main Landing Gears for UAV under Impact Loading*. ICAMSME 2015 (International Conference on Advanced Materials, Structures and Mechanical Engineering), South-Korea, May 29-31, 2015.

[6] Matta, A. K., Kumar, G. V. and Kumar, R. V., *Design Optimisation Of Landing Gear's Leg For An Un-Manned Aerial Vehicle*. International Journal of Engineering Research and Applications (IJERA), July-August, 2012, Vol.2, No.4, pp.2069-2075.

[7] Seshadri, P. and Parks, G. T., *Density-Matching for Turbomachinery Optimization Under Uncertainty*, arXiv Preprint arXiv:1510.04162, 2015. DOI: 10.1016/j.cma.2016.03.006

[8] Schëller, G.I. and Jensen, H.A., *Computational methods in optimization considering uncertainties An overview*. Computer Methods in Applied Mechanics and Engineering, 2008, Vol.198, pp.2-13. DOI: 10.1016/j.cma.2008.05.004

[9] Beyer, H-G and Sendhoff, B., *Robust optimization A comprehensive survey*. Computer Methods in Applied Mechanics and Engineering, 2007, Vol.196, pp.3190âĂŞ3218. DOI: 10.1016/j.cma.2007.03.003

[10] Lü, H. and Yu, D., *Stability Optimization of a Disc Brake System with Hybrid Uncertainties for Squeal Reduction*. Hindawi Publishing Corporation Shock and Vibration, 2016, Article ID 3497468. DOI: 10.1155/2016/3497468

[11] Xue, C. J., Dai, J. H., Wei, T. and Liu, B., *Structural Optimization of a Nose Landing Gear Considering its Fatigue Life*. JOURNAL OF AIRCRAFT, Vol. 49, No. 1, January-February, 2012. DOI: 10.2514/1.C031494.

[12] Goelke, M., *Multi-Disciplinary Design of an Aircraft Landing Gear with Altair HyperWorks*, Altair HyperWorks, October, 2008.

[13] Sobol', I. M., *Global sensitivity indices for nonlinear mathematical models and their Monte Carlo estimates*, Mathematics and Computers in Simulation, 2001, Vol.55, pp 271-280. DOI: 10.1016/S0378-4754(00)00270-6.

[14] Seshadri, P. Constantine, P. Iaccarino G. and Parks G, *Aggressive design: A density-matching approach for optimization under uncertainty*, Submitted to CMAME, September 26, 2014.

[15] Lopez, R. H. Torii, A.J., Miguel, L.F.F. and De Cursi, J.E.S., *An approach for the global reliability based optimization of the size and shape of truss structures.*, Mechanics & Industry, 2015, 16, 603.

[16] McDonald, M. and Mahadevan, S., *Design Optimization With System-Level Reliability Constraints.*, Journal of Mechanical Design, 2008, volume 130, number 2.

[17] Padulo, M. Campobasso, M. S. and Guenov, M. D., *Novel uncertainty propagation method for robust aerodynamic design*, AIAA JOURNAL, Vol.49, n.3, 2011, March. DOI: 10.2514/1.J050448

[18] Saltelli, A., Ratto, M., Andres, T., Campolongo, F., Cariboni, J., Gatelli, D., Saisana, M., and Tarantola, S., *Global Sensitivity Analysis, The Primer*. Wiley, 2008. DOI: 10.1002/9780470725184

[19] Tartaruga, I., Cooper, J. E., Lowenberg, M. H., Sartor, P. and Lemmens, Y., *Uncertainty and Sensitivity Analysis of Bifurcation Loci Characterizing Nonlinear Landing Gear Dynamics*, Journal of Aircraft, 2017, accepted manuscript and exported to production to begin the publication process on the 30/05/2017.

[20] Das, S. and Suganthan, P. N., *Differential Evolution: A Survey of the State-of-the-Art*, IEEE Transactions on Evolutionary Computation, Vol. 15, No.1, 2011. DOI: 10.1109/TEVC.2010.2059031

[21] Hegerty, B., Hung, C-C and Kasprak, K., *A Comparative Study on Differential Evolution and Genetic Algorithms for Some Combinatorial Problems*, 1st Workshop on Intelligent Methods in Search and Optimization (WIMSO), 2009.

[22] Swagatam, D., Ajith, A., and Amit, K., editor L. Ying, S. Aixin, L. Han Tong, L. Wen Feng, L. Ee-Peng, Chapter: Particle Swarm Optimization and Differential Evolution Algorithms: Technical Analysis, Applications and Hybridization Perspectives, *Advances of Computational Intelligence in Industrial Systems*, 2008, Springer Berlin Heidelberg, Berlin, Heidelberg, pp. 1-38, DOI 10.1007/978-3-540-78297-1_1, url=http://dx.doi.org/10.1007/9783540782971_1.

[23] Worden K., Staszewski W. J. and Hensman J. J., *Natural Computing for Mechanical Systems Research: A Tutorial Overview*, Mechanical Systems and Signal Processing, Vol.25, No.1, pp 4-111, 2011. DOI: 10.1016/j.ymssp.2010.07.013

[24] Khan M., Chaudhry I. A., Khan A. A. and Mahmood S., *Spreadsheet based genetic algorithm approach to optimize preliminary aircraft design*, Journal of scientific and industrial research 73(5):302-307 Âů May 2015.

[25] Brest, J., Zamuda, A., Fister, I., and Boskovic, B., *Some Improvements of the Self-Adaptive jDE Algorithm*, IEEE, 2014. DOI: 10.1109/SDE.2014.7031537

[26] Storn, R. and Price, K., *Differential evolution - a simple and efficient heuristic for global optimization over continuous spaces*, Journal of Global Optimization, Vol.11, No.4, pp. 341-359. DOI: 10.1023/A:1008202821328

[27] Tartaruga, I., Cooper, J. E., Lowenberg, M. H. and Sartor, P., Coggon, S. and Lemmens, Y., *Prediction and Uncertainty Propagation of Correlated Time-Varying Quantities using Surrogate Models*, CAES Aeronautical Journal, 7(1), pp 2942, 2016. DOI 10.1007/s13272-015-0172-1

[28] Tartaruga, I., Cooper, J. E., Sartor, P., and Lowenberg, M. H., and Coggon, S., and Lemmens, Y., *Efficient Prediction and Uncertainty Propagation of Correlated Loads*, SCITECH2015, January 5-8, Orlando, Florida USA, 2015. DOI: 10.2514/6.2015-1847

[29] Tartaruga, I., Cooper, J. E., and Lowenberg, M. H., Sartor, P. and Lemmens, Y., *Evaluation and Uncertainty Quantification of Bifurcation Diagram: Landing Gear, a case study*, UNCECOMP, May 25-27, Crete, Greece, 2015. DOI: 10.7712/120215.4307.512

[30] Tartaruga, I., Cooper, J. E., Lowenberg, M. H., Sartor, P. and Lemmens, Y., *Geometrical Based Method for the Uncertainty Quantification of Correlated Aircraft Loads*, ASDJournal Vol.4, No.1, May, 2016.

DOI: 10.3293/asdj.2016.40

[31] Chen, X., Molina-Cristbal, A., Guenov, M. D., Datta, V. C. and Riaz, A., *A novel method for inverse uncertainty propagation*, EUROGEN 2015, Glasgow, UK, September 2015. DOI: 10.1007/978-3-319-89988-6_21

[32] Price, K., Storn, R., and Lampinen, J., *Differential Evolution: A Practical Approach to Global Optimization*, Springer, Natural Computing Series, 2005. DOI: 10.1007/3-540-31306-0

[33] Mishra, Sudhanshu. "Some new test functions for global optimization and performance of repulsive particle swarm method". MPRA, 23rd august 2006. http://mpra.ub.uni-muenchen.de/2718/.

[34] Tartaruga, I. , *On the development of methodologies to deal with uncertainties in complex aeronautical systems*, Dissertation submitted to the University of Bristol, Department of Aerospace Engineering University of Bristol, April 2017.

[35] Tartaruga, I., Lemmens, Y., Sartor, P., Lowenberg, M. H. and Cooper, J. E., *On the influence of longitudinal tyre slip dynamics on aircraft landing gear shimmy*, USD2016 conferences, September 19-21, Leuven, Belgium, 2016.

[36] Tartaruga, I., Lowenberg, M. H., Cooper, J. E., Sartor, P. and Lemmens, Y., *Bifurcation Analysis of a Nose Landing Gear System*, SCITECH2016, January, San Diego, California, USA, 2016. DOI: 10.2514/6.2016-1572

[37] Guckenheimer, J., and Holmes, P., *Nonlinear Oscillations and Dynamical Systems and Bifurcations of Vector Fields*. Springer, Series Applied Mathematical Sciences, Vol. 42, 1983. DOI: 10.1002/zamm.19860660104

[38] Strogatz, S. H., *Nonlinear Dynamics And Chaos: With Applications To Physics, Biology, Chemistry, And Engineering Studies in Nonlinearity*. Westview Press, Studies in Nonlinearity, 2014.

[39] ICAO Doc 8168 PANS-OPS Vol 1, http://www.ce560xl.com/files downloaded in 2015.

[40] Doedel, E., and Oldeman, B., *Auto-07p: Continuation and Bifurcation Software*, 2012. http://www.dam.brown.edu/people/sandsted/auto/auto07p.pdf downloaded in November, 2014.

[41] http://seis.bris.ac.uk/ ec1099/, date accessed November, 2015.

[42] Howcroft, C., Krauskopf, B., Lowenberg, M. H., and Neild, S. A.,*Influence of Variable Side-Stay Geometry on the Shimmy Dynamics of an Aircraft Dual-Wheel Main Landing Gear*, SIAM Journal on Applied Dynamical Systems, vol 12., pp. 1181-1209, 2013. DOI: 10.1137/120887643

[43] Pacejka, Hans B., *Tyre and vehicle dynamics*, Second Edition, 2006 Elsevier Ltd.